

An efficient RBF-FD method using polyharmonic splines alongside polynomials for the numerical solution of two-dimensional PDEs held on irregular domains and subject to Dirichlet and Robin boundary conditions

Asghar Rahimi, Elyas Shivanian*

Department of Applied Mathematics, Imam Khomeini International University, Qazvin, 34149-16818, Iran

(Communicated by Haydar Akca)

Abstract

In the present paper, the relatively new method of Radial Basis Function-Generated Finite Difference (RBF-FD) is used to solve a class of Partial Differential Equations (PDEs) with Dirichlet and Robin boundary conditions. For this approximation, Polyharmonic Splines (PHS) are used alongside Polynomials. This combination has many benefits. On the other hand, Polyharmonic Splines have no shape parameter and therefore relieve us of the hassle of calculating the optimal shape parameter. As the first problem, a two-dimensional Poisson equation with the Dirichlet boundary condition is investigated in various domains. Then, an elliptic PDE with the Robin boundary condition is solved by the proposed method. The results of numerical studies indicate the excellent efficiency, accuracy and high speed of the method, while for these studies, very fluctuating and special test functions have been used.

Keywords: Partial Differential Equations, Radial basis functions, Polyharmonic Splines, Robin boundary condition, RBF-FD

2010 MSC: 65N99

1 Introduction

A significant part of the numerical analysis literature, is devoted to the numerical solution of PDEs. In the past decades, a wide variety of methods have been developed to solve these equations. Some researchers believe that Finite Difference Method (FDM), Finite Element Method (FEM) and Spectral methods are three macro strategies for numerical solution of PDEs. FDM and FEM are very well-known and widely used methods. Spectral methods have also proven their abilities in solving various problems, including Fractional Differential Equations (FDEs), Delay Differential Equations (DDEs), and nonlinear problems [5, 6, 7, 8, 34, 54].

However, due to some problems especially in scattered nodes approximation, in recent years, a new generation of numerical methods have emerged, which are referred to as Meshless methods, and are becoming the fourth major strategy. The main attractiveness of the Meshless methods is due to their high flexibility in solving problems with

*Corresponding author

Email addresses: a.rahimi@edu.ikiu.ac.ir (Asghar Rahimi), shivanian@sci.ikiu.ac.ir (Elyas Shivanian)

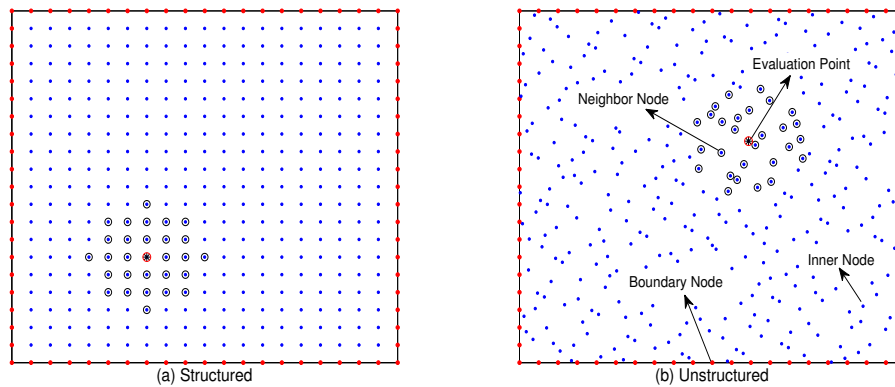


Figure 1: Two stencils consisting of 29 nodes on two different node distributions.

higher dimensions, complex geometries and irregular or unstructured node distributions [1, 35, 41, 45]. Radial basis functions play a vital role in these methods because of their ability to interpolate and approximate scattered data [21, 27, 28, 30, 32, 33, 42, 52, 53].

The RBF-FD method, is a young method that has been established in the last two decades [46, 49, 50]. This method, with the help of RBFs, approximates the weights of finite differences for local domains, in such a way that it can be applied on scattered nodes and any spatial dimension desired [9].

The RBF-FD method can be implemented in different situations, especially in large-scale actual problems and this is one of the prominent features of this method. In [37], an adaptive RBF-FD scheme is used to solve elliptic problems with point singularities. A high dimensional time fractional convection-diffusion equation, is investigated in [38] using the RBF-FD method. This method is also used for solution of GKdVB equation in [40]. The method is applied to thoracic diaphragm simulations in [51]. Atmospheric flow, Navier-Stokes equations and Shan-Chen model are also analyzed in [2, 24, 48]. For more information on other features of the method, one can refer to [18, 27, 29, 43] and references therein.

In the structure of the method, different RBFs could be used. Infinitely smooth RBFs have been used in several articles, especially in the early years of the method [11, 14, 19, 25, 47]. The use of this type of functions, in addition to its good features, will also have limitations such as calculating the optimal shape parameter [12, 13, 22, 26]. In recent years, good studies have been conducted on the role of polynomials and polyharmonic splines in the RBF-FD method [15, 17, 23]. The results of these studies indicate that combining polynomials with polyharmonic splines has great advantages and relieves us of the limitations we had in the RBF-FD methods based on infinitely smooth RBFs [9, 16]. For example, in some RBF-FD methods that use radial functions with the shape parameter such as Multiquadrics [12, 13] or Inverse Quadratics [39], sometimes we have to use symbolic computation to find the optimal value of this parameter, which is costly. It was mentioned that this problem had been solved in the proposed method. On the other hand, suitable features of RBF-FD methods like sparsity, geometric flexibility and easy implementation are still maintained in this combination. The PHS+poly-based RBF-FD method is a well-established numerical procedure that could be applied to various complicated issues. For instance in [15], excellent performance of the method for some challenging test cases, and for some equations that are close to actual application is shown. Therefore, in this paper we will use this fresh and improved version of RBF-FD method which is based on PHS augmentation with polynomials, to solve some elliptic PDEs.

In Section 2, the method will be described in detail. In Section 3, using special test functions, the method will be analyzed on the two-dimensional Poisson equation in different domains, with different degrees of polynomials and different PHS functions. Then, with the help of the obtained results, in section 4, an elliptic PDE with the Robin boundary condition will be examined. To highlight the capabilities of the method, highly oscillatory coefficients and test functions will be used. Finally, important results and suggestions for future works will be presented.

2 RBF-FD method using Polyharmonic Splines alongside Polynomials

As mentioned before, the RBF-FD method works locally. Consider the node $\mathbf{x} = \mathbf{x}^*$ in a problem domain. Using $\mathbf{x} = \mathbf{x}^*$ and $(n - 1)$ nodes surrounding it, we will form a stencil consisting of n distinct nodes. These stencils could be in any shape for each node (refer to Fig. 1). To approximate a linear operator such as the differential operator $\mathcal{L}[\cdot]$ at the point $\mathbf{x} = \mathbf{x}^*$, we can use a linear combination of the values of $u(\mathbf{x})$ at the points forming the stencil of $\mathbf{x} = \mathbf{x}^*$ as follows:

$$\mathcal{L}[u(\mathbf{x}^*)] \approx \sum_{i=1}^n w_i u(\mathbf{x}_i), \tag{2.1}$$

in which $\{w_i\}_{i=1}^n$ are the unknown weights and n is the stencil size. In calculating conventional Finite Difference formulas, one of the simplest algorithms to find the unknown weights is to use polynomial interpolation. A special change in the RBF-FD method, is the use of radial functions for finding the unknown weights. Therefore computing the unknown weights in the RBF-FD manner, unlike the classical FD, is not grid-based and can be easily applied on scattered nodes and dimensions of more than one [27].

Suppose the interpolant $s(\mathbf{x})$ of the form:

$$s(\mathbf{x}) = \sum_{i=1}^n \alpha_i \phi(r_i(\mathbf{x})) + \sum_{j=1}^k \beta_j p_j(\mathbf{x}), \tag{2.2}$$

where $r_i(\mathbf{x}) = \|\mathbf{x} - \mathbf{x}_i\|$, is the standard Euclidean distance between the point of interest \mathbf{x} and a node at \mathbf{x}_i and $\phi(r_i(\mathbf{x}))$ is an RBF centered on \mathbf{x}_i . In this article, we have used PHS functions as RBFs which are of the form:

$$\phi(r) = r^{2m-1}, \quad m \in \mathbb{N}. \tag{2.3}$$

It is remarkable that, if the Highest Polynomial Degree (HPD) desired to include in the d -dimensional method, is $HPD = l$, then $\{p_j(\mathbf{x})\}_{j=1}^k$ is a basis polynomials up to degree l in d dimensions with $k = \binom{l+d}{l}$. For instance, if $d = 2$ and $l = 3$, then $k = \binom{3+2}{3} = 10$, and the polynomial basis would be of the form:

$$\{ 1, x, y, x^2, xy, y^2, x^3, x^2y, xy^2, y^3 \}. \tag{2.4}$$

Enforcing the Eq.(2.1) to be exact for the interpolant $s(\mathbf{x})$ with matching constraints:

$$\sum_{i=1}^n \alpha_i p_j(\mathbf{x}_i) = 0, \quad j = 1, 2, 3, \dots, k, \tag{2.5}$$

yields the following linear system:

$$\begin{bmatrix} \mathbf{A} & \mathbf{P} \\ \mathbf{P}^T & \mathbf{0} \end{bmatrix} \begin{bmatrix} \mathbf{w} \\ \mathbf{v} \end{bmatrix} = \begin{bmatrix} \mathbf{b} \\ \mathbf{c} \end{bmatrix}. \tag{2.6}$$

The components of the above system are as follows:

$$\mathbf{A} = \begin{bmatrix} \phi(\|\mathbf{x}_1 - \mathbf{x}_1\|) & \phi(\|\mathbf{x}_1 - \mathbf{x}_2\|) & \dots & \phi(\|\mathbf{x}_1 - \mathbf{x}_n\|) \\ \phi(\|\mathbf{x}_2 - \mathbf{x}_1\|) & \phi(\|\mathbf{x}_2 - \mathbf{x}_2\|) & \dots & \phi(\|\mathbf{x}_2 - \mathbf{x}_n\|) \\ \vdots & \vdots & \ddots & \vdots \\ \phi(\|\mathbf{x}_n - \mathbf{x}_1\|) & \phi(\|\mathbf{x}_n - \mathbf{x}_2\|) & \dots & \phi(\|\mathbf{x}_n - \mathbf{x}_n\|) \end{bmatrix}_{n \times n}, \tag{2.7}$$

$$\mathbf{P} = \begin{bmatrix} p_1(\mathbf{x}_1) & p_2(\mathbf{x}_1) & \dots & p_k(\mathbf{x}_1) \\ p_1(\mathbf{x}_2) & p_2(\mathbf{x}_2) & \dots & p_k(\mathbf{x}_2) \\ \vdots & \vdots & \ddots & \vdots \\ p_1(\mathbf{x}_n) & p_2(\mathbf{x}_n) & \dots & p_k(\mathbf{x}_n) \end{bmatrix}_{n \times k}, \tag{2.8}$$

$$\mathbf{w}^T = [w_1 \quad w_2 \quad \dots \quad w_n]_{1 \times n}, \tag{2.9}$$

$$\mathbf{v}^T = [v_1 \quad v_2 \quad \dots \quad v_k]_{1 \times k}, \quad (2.10)$$

$$\mathbf{b}^T = [L\phi(\|\mathbf{x}^* - \mathbf{x}_1\|) \quad L\phi(\|\mathbf{x}^* - \mathbf{x}_2\|) \quad \dots \quad L\phi(\|\mathbf{x}^* - \mathbf{x}_n\|)]_{1 \times n}, \quad (2.11)$$

$$\mathbf{c}^T = [Lp_1(\mathbf{x}^*) \quad Lp_2(\mathbf{x}^*) \quad \dots \quad Lp_k(\mathbf{x}^*)]_{1 \times k}. \quad (2.12)$$

The unknown weights $\{w_i\}_{i=1}^n$, could be find by solving the system (2.6). It is worth saying that the weights contained in \mathbf{v} would be disregarded after solving the system.

In summary, the steps for implementing the RBF-FD method on a PDE, can be listed as follows:

- (i) Node generation;
- (ii) Defining for each evaluation point, a stencil consisting of some neighbor nodes;
- (iii) Constructing an approximation for each differential operator, using a linear combination of the values of the unknown function at the nodes scattered in the stencil;
- (iv) Computing the *weights* or differencing coefficients for each stencil;
- (v) Substituting the earned approximations in step (iv) for derivatives, at each node in the PDE, to earn the corresponding final system;
- (vi) Solving the final global system.

Several factors could affect the accuracy of RBF-FD methods. For example, to find the neighbor nodes concluded in each stencil, different algorithms could be used. Here we have used the *Matlab* command *knnsearch* for this purpose. In the method proposed here, determining the following three items, also play an important role in the robustness of the method:

- (i) The number of nodes included in each stencil or stencil size;
- (ii) The kind of PHS radial function;
- (iii) The highest degree of polynomial should be included to support the approximation.

We analyze these triple items in our numerical investigations. It is notable that in the current paper we represent the stencil size with n , the PHS radial function with $\phi(r)$ and the highest polynomial degree included, with HPD. Besides, showing the efficiency of the method, the following root mean square (RMS) error is used:

$$\text{RMS error} = \sqrt{\frac{\sum_{i=1}^N (u_{exact}(\mathbf{x}_i) - \hat{u}(\mathbf{x}_i))^2}{N}}, \quad (2.13)$$

where $u_{exact}(\mathbf{x}_i)$ and $\hat{u}(\mathbf{x}_i)$ are achieved by exact and approximate solutions on points \mathbf{x}_i and N is number of nodal points.

In sections 3 and 4, for the numerical experiments, we will use the following problem domains in two structured and unstructured forms of node distributions:

$$\Omega_1 = \{ (x, y) \mid 0 \leq x, y \leq 1 \}, \quad (2.14)$$

$$\Omega_2 = \{ (x, y) \mid x^2 + y^2 \leq 1 \}, \quad (2.15)$$

and

$$\Omega_3 = \{ (x, y) \mid 0 \leq x, y \leq 1 \text{ and } (x - 0.5)^2 + (y - 0.5)^2 \geq 0.09 \}. \quad (2.16)$$

Some examples of these domains are plotted in Fig. 2. Halton points are used in unstructured node distributions. This type of distributions as well as the diversity of the used domains, show the geometric flexibility of the method.

At the end of this part, the algorithmic form of the steps to approximate the RBF-FD weights for each node, is presented as follows:

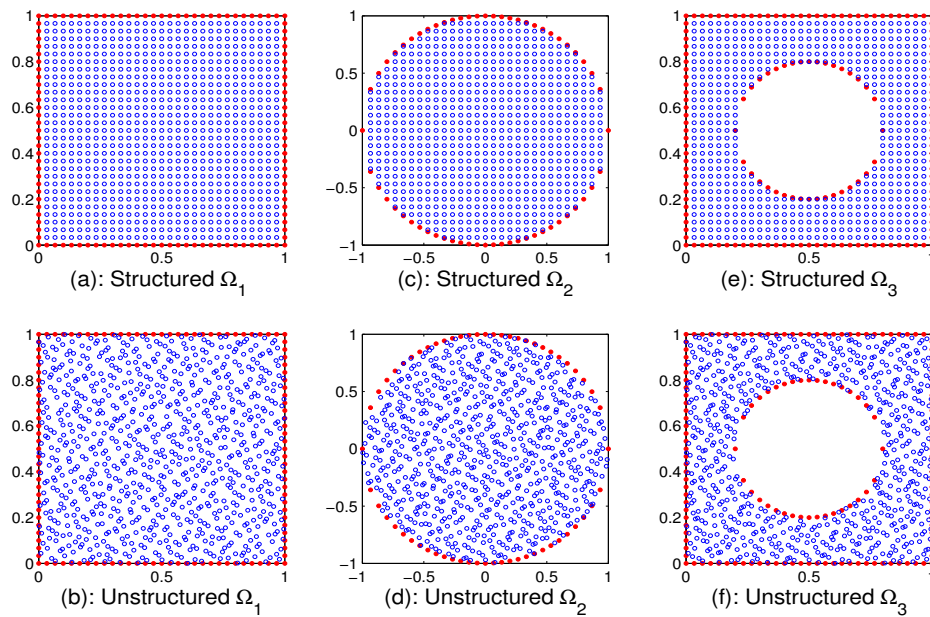


Figure 2: Examples of problem domains considered for test functions in the current paper. Unstructured node distributions are generated using Halton nodes.

- **Input** n , $\phi(r)$ and HPD.
- **Step1.** Compute the entries of the matrices \mathbf{A} (2.7), \mathbf{P} (2.8) and also the entries of the vectors \mathbf{b} (2.11) and \mathbf{c} (2.12).
- **Step2.** Solve the system (2.6).
- **Output** \mathbf{w} (2.9).

It should be noted that all the codes used to extract the numerical results, were written and implemented using Matlab R2013b in a system with the following specifications:

ASUS X555LPB, Processor: Intel(R) Core(TM) i7-5500U CPU 2.40GHz, RAM: 6 GB, Storage space: 931.51 GB.

3 Analysis of the proposed RBF-FD method on a two-dimensional Poisson equation in different problem domains

The problem and the examples considered here in Section 3, have already been studied by several researchers using different methods. Among them are [12] and [53], which use RBF-FD methods based on multiquadrics and RBF-HFD method. In the methods based on radial functions with shape parameters, calculation of the optimal shape parameter is very important and of course this is associated with some difficulties. In the current method, we could get good answers in various domains without these difficulties. Our studies show that the method presented here, could be applied to various problems with high accuracy and speed.

In this section, we will analyze the method on a two-dimensional Poisson problem, which is defined as follows:

$$\Delta u = f \text{ in } \Omega, \quad u = g \text{ on } \partial\Omega, \quad (3.1)$$

in which Δ is the Laplace linear differential operator and f and g are computed using the known exact solution.

Table 1: The RMS error for the problem (3.1) with the known solution (3.2) on Ω_1 using Halton nodes. Besides $N=1681$, $n=31$ and the results for different PHS radial functions and HPDs are reported.

$\phi(r)$ HPD	3	4	5
r^3	8.05427e-04	4.47451e-05	2.53787e-05
r^5	2.38292e-04	1.52933e-05	8.03749e-06
r^7	6.02989e-05	7.50932e-06	5.03431e-06

Table 2: The RMS error for the problem (3.1) with the known solution (3.2) on Ω_1 .

Structured: $\phi(r) = r^7$, HPD=7, $n=101$			Unstructured: $\phi(r) = r^7$, HPD=7, $n=71$		
N	RMS error	CPU Time	N	RMS error	CPU Time
1681	7.65350e-08	38.26	121	3.30527e-04	1.02
2601	1.85246e-08	59.88	441	3.84192e-06	3.99
3721	6.05416e-09	86.73	961	1.90809e-07	8.89
5041	2.43173e-09	120.78	1681	2.72294e-08	15.73

3.1 First Example

Suppose the function:

$$u(x, y) = \sin(\pi x)\cos(2\pi y)e^{-(x-\frac{1}{4})^2-(y-\frac{1}{2})^2}, \tag{3.2}$$

as the first test function for the problem (3.1). We have applied the method for the function (3.2), on two different problem domains Ω_1 and Ω_3 (refer to Fig. 2). The results are described below in detail.

In Table 1, the RMS error for the problem (3.1) with the known solution (3.2), using 1521 Halton nodes in Ω_1 and 160 structured nodes on $\partial\Omega_1$ is reported. The stencil size is $n = 31$ and the results for different PHS RBFs and different levels of polynomials are expressed. Note that with proportional changes in the radial function and the degree of the polynomial, more accurate results could be obtained. To better understand the effect of these changes, refer to Fig. 3.

Our studies show that, the role of polynomials is more prominent than PHS radial functions and stencil size. Also, similar results are reported in [9]. To explore the fact, in Fig. 3, the RMS errors of the problem (3.1) with the known solution (3.2) on Ω_1 , for different stencil sizes and for increasing number of total nodes N is represented. The node generation is unstructured and Halton nodes are used here again. As it is clear from the figure, by changing the degree of the polynomial, the accuracy of the answer is severely affected and the slope of the error curve changes. But by changing the radial function, the slope does not change almost, and the error curve goes a little higher or lower. Stencil resizing is also less effective than the other two factors. Besides, while the number of total nodes increases, the errors are decreasing.

In Table 2, the RMS error of the problem (3.1) with the known solution (3.2) on Ω_1 for both structured and unstructured node distributions and the different number of total nodes is brought. In this table and the further tables, the CPU time is also reported in seconds. Table 3 is same as Table 2 but for Ω_3 . Both tables show the accuracy and power of the method to solve the problem, even in irregular domains and node distributions.

Table 3: The RMS error for the problem (3.1) with the known solution (3.2) on Ω_3 .

Structured: $\phi(r) = r^7$, HPD=6, $n=91$			Unstructured: $\phi(r) = r^7$, HPD=6, $n=31$		
N	RMS error	CPU Time	N	RMS error	CPU Time
214	1.29272e-04	2.17	420	7.12328e-06	0.79
534	1.53429e-05	5.91	845	2.25808e-06	1.77
1288	2.96984e-07	15.54	1416	4.77374e-07	2.78
1610	3.53384e-07	21.41	2129	2.25974e-07	4.61

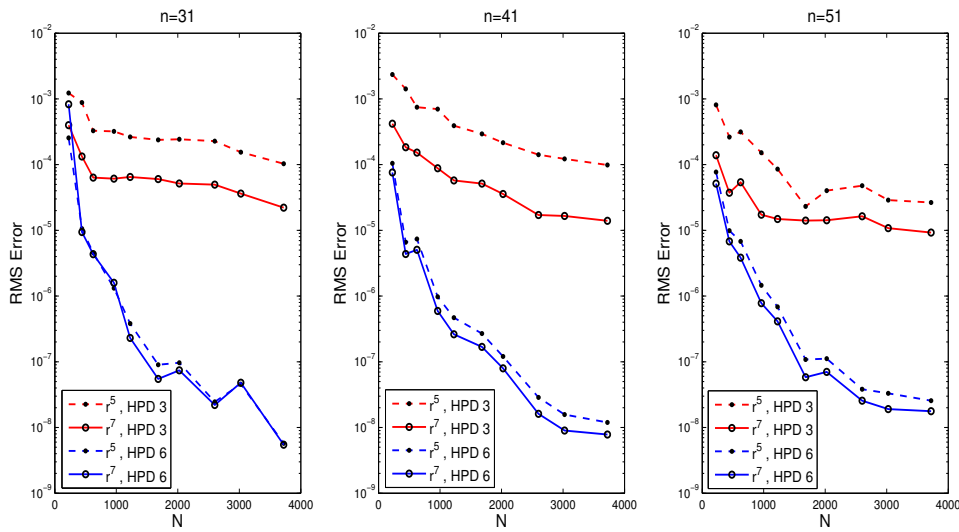


Figure 3: The effect of stencil resizing, changing the radial function and the highest polynomial degree included, on the accuracy of the answer for the problem (3.1) with the known solution (3.2), while the number of total nodes N is increasing.

Table 4: The RMS error for the problem (3.1) with the known solution (3.3) on Ω_2 .

Structured: $\phi(r) = r^7$, HPD=7, $n=101$			Unstructured: $\phi(r) = r^7$, HPD=7, $n=81$		
N	RMS error	CPU Time	N	RMS error	CPU Time
757	2.35125e-12	13.87	817	4.19991e-12	9.10
2041	1.14965e-14	42.17	2144	1.77112e-13	23.81
3981	1.07612e-15	84.14	4098	4.16535e-14	47.33
6529	3.06171e-16	141.70	6683	6.13439e-15	81.05

3.2 Second Example

Now we will perform the method for the problem (3.1) with the new test function:

$$u(x, y) = \frac{25}{25 + (x - 0.2)^2 + 2y^2} \quad (3.3)$$

in the unit disk Ω_2 .

In Table 4, the RMS error of the problem (3.1) with the known solution (3.3) on Ω_2 for both structured and unstructured node distributions and the different number of total nodes is shown. The results, show the robustness of the method, and the errors earned here, are better than the errors reported in [53].

4 The method implementation on two-dimensional elliptic PDEs with Robin boundary condition

In this section, using the information earned from the analysis of the proposed method in Section 3, we will perform the method on the following problem:

$$\begin{cases} \Delta u + u = f, & \text{in } \Omega, \\ \frac{\partial u}{\partial \mathbf{n}} + p \cdot u = g, & \text{on } \partial\Omega, \end{cases} \quad (4.1)$$

where Δ is the Laplace linear differential operator, f and g are computed using the known exact solution, \mathbf{n} is the outward unit normal on the boundary $\partial\Omega$ and p would be given as a coefficient function.

Table 5: The RMS error for the problem (4.1) with the known solution (4.2) on Ω_1 .

Structured: $\phi(r) = r^5, \quad \text{HPD}=2, \quad n=31$			Unstructured: $\phi(r) = r^5, \quad \text{HPD}=2, \quad n=25$		
N	RMS error	CPU Time	N	RMS error	CPU Time
441	4.34194e-13	0.95	441	8.32795e-13	0.77
961	2.56154e-13	2.13	961	4.63491e-13	1.67
1681	1.92028e-12	3.75	1681	9.44722e-13	2.56
2601	1.86218e-12	5.88	2601	6.18215e-13	4.34

Shivanian in [44], has analyzed the problem (4.1) using the PSMRPI and PSMRPHI techniques. There are also other papers, such as [3, 4, 20, 31], in which the problem (4.1) has been solved using different methods. It is remarkable that in [10] and [36], the existence and uniqueness of the solution of the problem (4.1) are explored.

In this section, we will implement the method in three examples. In all numerical experiments, the problem domain Ω_1 , with both structured and unstructured node distributions, is used. To better show the power of the method, we will use highly oscillatory test functions and also coefficient functions in the boundary condition.

4.1 First Example

Suppose the following function as the first model problem:

$$u(x, y) = 2x + y + 1, \quad (4.2)$$

besides consider the coefficient function in the boundary condition as:

$$p(x, y) = 81x. \quad (4.3)$$

Note that, for a node such as \mathbf{x}_i on the boundary $\partial\Omega_1$, the outward unit normal is defined as follows:

$$\mathbf{n} = n_1(\mathbf{x}_i)\mathbf{i} + n_2(\mathbf{x}_i)\mathbf{j} \quad (4.4)$$

and therefore $\frac{\partial u}{\partial \mathbf{n}}$ would be of the form:

$$\frac{\partial u}{\partial \mathbf{n}} = n_1(\mathbf{x}_i)\frac{\partial u(\mathbf{x}_i)}{\partial x} + n_2(\mathbf{x}_i)\frac{\partial u(\mathbf{x}_i)}{\partial y}. \quad (4.5)$$

Now, using the exact solution (4.2), the coefficient function (4.3), and the preceding relations, we can calculate the right-hand side of the problem (4.1) and also the right-hand side of the boundary condition.

In Table 5, the RMS error of the problem (4.1) with the known solution (4.2) on Ω_1 for both structured and unstructured node distributions and the different number of total nodes is shown. It was predictable that the errors earned from the approximation for this example, would be very low. Because the exact solution (4.2) and also the coefficient function (4.3) are easy polynomials.

4.2 Second Example

Suppose the following function as the second model problem:

$$u(x, y) = \sin(\pi x)\sin(\pi y), \quad (4.6)$$

and also consider the following:

$$p(x, y) = x^2y. \quad (4.7)$$

In Table 6, the RMS error of the problem (4.1) with the known solution (4.6) on Ω_1 for both structured and unstructured node distributions and the different number of total nodes is shown. It can be seen that even with a significant increase in the number of points, the computational efficiency in terms of execution time is acceptable.

Table 6: The RMS error for the problem (4.1) with the known solution (4.6) on Ω_1 .

Structured: $\phi(r) = r^5$, HPD=2, $n=51$			Unstructured: $\phi(r) = r^5$, HPD=2, $n=31$		
N	RMS error	CPU Time	N	RMS error	CPU Time
5041	5.26674e-03	27.10	5041	1.57956e-03	13.56
6561	4.01846e-03	39.03	6561	1.76129e-04	19.68
8281	3.29422e-03	52.72	8281	9.75582e-05	28.82
10201	2.55551e-03	71.48	10201	5.23174e-04	42.91

Table 7: The RMS error for the problem (4.1) with the known solution (4.8) on Ω_1 .

Structured: $\phi(r) = r^7$, HPD=3, $n=71$			Unstructured: $\phi(r) = r^7$, HPD=3, $n=61$		
N	RMS error	CPU Time	N	RMS error	CPU Time
2601	3.29733e-04	25.78	441	2.71953e-03	3.63
3721	1.85728e-04	37.01	961	1.89856e-04	7.22
5041	1.13979e-04	51.49	1681	8.80267e-05	12.44
6561	8.20834e-05	68.73	2601	9.90478e-05	19.26

4.3 Third Example

Now, as the last example, consider the following test function:

$$u(x, y) = \frac{\arctan(2(x + 3y - 1))}{\arctan(2(\sqrt{10} + 1))}, \quad (4.8)$$

and highly oscillatory coefficient function:

$$p(x, y) = e^{(-y^2 + \cos(4\pi x)\sin(3\pi y))}. \quad (4.9)$$

Same as the other examples, in Table 7, the RMS error of the problem (4.1) with the known solution (4.8) on Ω_1 for both structured and unstructured node distributions and the different number of total nodes is shown. The errors and CPU times are perfect and acceptable for this particular example.

5 Conclusion

In the current paper, a very efficient version of the RBF-FD method is used to solve some PDEs. In this formulation, polynomials and polyharmonic splines are used together to approximate the unknown weights. The most important advantages of this combination are eliminating the computational complexity of the previous methods in finding the optimal shape parameter, and also to increase the speed and accuracy of the approximation. In this article, we first applied the proposed method to a Poisson problem with Dirichlet boundary conditions in regular and irregular domains, as well as on the structured and unstructured distribution of nodes. The performance of the method was compared in these different situations, and the earned results showed high strength and accuracy of the method in all conditions. In the next step, we applied the method to a two-dimensional boundary value problem with Robin boundary conditions. The implementation of the method was compared in two different node distributions. The accuracy of the results and the speed of the calculations, compared to the methods that use radial functions dependent on a shape parameter, were very suitable, even for more challenging and highly oscillatory examples. For future works, it would be suggested the method experiment on nonlinear problems or other complicated situations such as biharmonic equations.

Acknowledgements

The authors are very grateful to anonymous reviewers for carefully reading the paper and for their comments and suggestions which have improved the paper very much.

References

- [1] S. Abbasbandy, E. Shivanian, K. Hammood AL-Jizani, and S.N. Atluri, *Pseudospectral meshless radial point interpolation for generalized biharmonic equation subject to simply supported and clamped boundary conditions*, Engin. Anal. Boundary Elements **125** (2021), 23–32.
- [2] M. Abbaszadeh, M. Dehghan, Simulation flows with multiple phases and components via the radial basis functions-finite difference (RBF-FD) procedure: Shan-Chen model, Engineering Analysis with Boundary Elements, 119 (2020) 151-161.
- [3] P. Assari, H. Adibi, and M. Dehghan, *A meshless discrete Galerkin (MDG) method for the numerical solution of integral equations with logarithmic kernels*, J. Comput. Appl. Math. **267** (2014), 160–181.
- [4] P. Assari and M. Dehghan, *A meshless discrete collocation method for the numerical solution of singular-logarithmic boundary integral equations utilizing radial basis functions*, Appl. Math. Comput. **315** (2017), 424–444.
- [5] A.G. Atta, W.M. Abd-Elhameed, G.M. Moatimid, and Y.H. Youssri, *Modal shifted fifth-kind Chebyshev tau integral approach for solving heat conduction equation*, Fractal Fractional **6** (2022), no. 11, 619.
- [6] A.G. Atta and Y.H. Youssri, *Advanced shifted first-kind Chebyshev collocation approach for solving the nonlinear time-fractional partial integro-differential equation with a weakly singular kernel*, Comp. Appl. Math. **41** (2022), no. 8, 381.
- [7] A.G. Atta, W.M. Abd-Elhameed, G.M. Moatimid, and Y.H. Youssri, *A fast Galerkin approach for solving the fractional Rayleigh-Stokes problem via sixth-kind Chebyshev polynomials*, Mathematics **10** (2022), no. 11, 1843.
- [8] A.G. Atta, W.M. Abd-Elhameed, and Y.H. Youssri, *Shifted fifth-kind Chebyshev polynomials Galerkin-based procedure for treating fractional diffusion-wave equation*, Int. J. Modern Phys. **33** (2022), no. 8, 2250102.
- [9] G.A. Barnett, *A robust RBF-FD formulation based on polyharmonic splines and polynomials*, Ph.D. thesis, University of Colorado, 2015.
- [10] G. Barton, *Elements of Green's Functions and Propagation: Potentials, Diffusion, and Waves*, Oxford University Press, New York, 1989.
- [11] V. Bayona, M. Moscoso, M. Carretero, and M. Kindelan, *RBF-FD formulas and convergence properties*, J. Comput. Phys. **229** (2010), 8281–8295.
- [12] V. Bayona, M. Moscoso, and M. Kindelan, *Optimal constant shape parameter for multiquadric based RBF-FD method*, J. Comput. Phys. **230** (2011), 7384–7399.
- [13] V. Bayona, M. Moscoso, and M. Kindelan, *Optimal variable shape parameter for multiquadric based RBF-FD method*, J. Comput. Phys. **231** (2012), 2466–2481.
- [14] V. Bayona, M. Moscoso, and M. Kindelan, *Gaussian RBF-FD weights and its corresponding local truncation errors*, Engin. Anal. Boundary Elements **36** (2012), 1361–1369.
- [15] V. Bayona, N. Flyer, B. Fornberg, and G.A. Barnett, *On the role of polynomials in RBF-FD approximations: II. Numerical solution of elliptic PDEs*, J. Comput. Phys. **332** (2017), 257–273.
- [16] V. Bayona, *An insight into RBF-FD approximations augmented with polynomials*, Comput. Math. Appl. **77** (2019), 2337–2353.
- [17] V. Bayona, N. Flyer, and B. Fornberg, *On the role of polynomials in RBF-FD approximations: III. Behavior near domain boundaries*, J. Comput. Phys. **380** (2019), 378–399.
- [18] M. Dehghan and V. Mohammadi, *A numerical scheme based on radial basis function finite difference (RBF-FD) technique for solving the high-dimensional nonlinear Schrödinger equations using an explicit time discretization: Runge–Kutta method*, Compu. Phys. Commun. **217** (2017), 23–34.
- [19] H. Ding, C. Shu, D. B. Tang, Error estimates of local multiquadric-based differential quadrature (LMQDQ) method through numerical experiments, Int. J. Numer. Methods Eng. **63** (2005), 1513–1529.
- [20] W. Fang, Y. Wang, and Y. Xu, *An implementation of fast wavelet Galerkin methods for integral equations of the second kind*, J. Sci. Comput. **20** (2004), 277–302.

- [21] G.E. Fasshauer, *Meshfree Approximation Methods with MATLAB*, Interdisciplinary Mathematical Sciences 6, World Scientific Publishers, Singapore, 2007.
- [22] G.E. Fasshauer and J.G. Zhang, *On choosing “optimal” shape parameters for RBF approximation*, Numer. Alg. **45** (2007), 345–368.
- [23] N. Flyer, B. Fornberg, V. Bayona, and G.A. Barnett, *On the role of polynomials in RBF-FD approximations: I. Interpolation and accuracy*, J. Comput. Phys. **321** (2016), 21–38.
- [24] N. Flyer, G.A. Barnett, and L.J. Wicker, *Enhancing finite differences with radial basis functions: Experiments on the Navier-Stokes equations*, J. Comput. Phys. **316** (2016), 39–62.
- [25] B. Fornberg and G. Wright, *Stable computation of multiquadric interpolants for all values of the shape parameter*, Comput. Math. Appl. **48** (2004), 853–867.
- [26] B. Fornberg and C. Piret, *On choosing a radial basis function and a shape parameter when solving a convective PDE on a sphere*, J. Comput. Phys. **227** (2008), 2758–2780.
- [27] B. Fornberg and N. Flyer, *A Primer on Radial Basis Functions with Applications to the Geosciences*, SIAM, Philadelphia, 2015.
- [28] B. Fornberg and N. Flyer, *Solving PDEs with radial basis functions*, Acta Numerica **24** (2015), 215–258.
- [29] D. Gunderman, N. Flyer, and B. Fornberg, *Transport schemes in spherical geometries using spline-based RBF-FD with polynomials*, J. Comput. Phys. **408** (2020), 109256.
- [30] R.L. Hardy, *Multiquadric equations of topography and other irregular surfaces*, J. Geophys. Res. **76** (1971), 1905–1915.
- [31] J. Helsing and A. Karlsson, *An explicit kernel-split panel-based Nystrom scheme for integral equations on axially symmetric surfaces*, J. Comput. Phys. **272** (2014), 686–703.
- [32] E.J. Kansa, *Multiquadrics—a scattered data approximation scheme with applications to computational fluid-dynamics I: Surface approximations and partial derivative estimates*, Comput. Math. Appl. **19** (1990), 127–145.
- [33] E.J. Kansa, *Multiquadrics—a scattered data approximation scheme with applications to computational fluid-dynamics II: Solutions to parabolic, hyperbolic and elliptic partial differential equations*, Comput. Math. Appl. **19** (1990), 147–161.
- [34] H.R. Khodabandehlo, E. Shivanian, and S. Abbasbandy, *Numerical solution of nonlinear delay differential equations of fractional variable-order using a novel shifted Jacobi operational matrix*, Engin. Comput. **38** (2022), 2593–2607.
- [35] G. Liu and Y. Gu, *An Introduction to Meshfree Methods and Their Programming*, Springer, 2005.
- [36] R. Nittka, *Elliptic and parabolic problems with Robin boundary conditions on Lipschitz domains*, Ph.D. Thesis, Universität Ulm, 2010.
- [37] D.T. Oanh, O. Davydov, and H.X. Phu, *Adaptive RBF-FD method for elliptic problems with point singularities in 2D*, Appl. Math. Comput. **313** (2017), 474–497.
- [38] Y. Qiao, S. Zhai, and X. Feng, *RBF-FD method for the high dimensional time fractional convection-diffusion equation*, Int. Commun. Heat Mass Transfer **89** (2017), 230–240.
- [39] A. Rahimi, C.A.E. Shivanian, and S. Abbasbandy, *Analysis of new RBF-FD weights, calculated based on inverse quadratic functions*, J. Math. **2022** (2022), Article ID 3718132, 7 pages.
- [40] J. Rashidinia and M.N. Rasoulizadeh, *Numerical methods based on radial basis function-generated finite difference (RBF-FD) for solution of GKdVB equation*, Wave Motion. **90** (2019), 152–167.
- [41] D. Rostamy, M. Emamjome, and S. Abbasbandy, *A meshless technique based on the pseudospectral radial basis functions method for solving the two-dimensional hyperbolic telegraph equation*, Eur. Phys. J. Plus **132** (2017), 1–11.
- [42] R. Schaback, *Error estimates and condition numbers for radial basis function interpolants*, Adv. Comput. Math. **3** (1995), 251–264.

- [43] V. Shankar, G.B. Wright, R.M. Kirby, and A.L. Fogelson, *A radial basis function (RBF)- finite difference (FD) method for diffusion and reaction-diffusion equations on surfaces*, J. Sci. Comput. **63** (2015), 745–768.
- [44] E. Shivanian, *Pseudospectral meshless radial point hermit interpolation versus pseudospectral meshless radial point interpolation*, Int. J. Comput. Meth. **17** (2020), no. 7, 1950023.
- [45] E. Shivanian, A. Rahimi, and M. Hosseini, *Meshless local radial point interpolation to three-dimensional wave equation with Neumann's boundary conditions*, Int. J. Comput. Math. **93** (2016), no. 12, 2124–2140.
- [46] C. Shu, H. Ding, K.S. Yeo, *Local radial basis function-based differential quadrature method and its application to solve two-dimensional incompressible Navier-Stokes equations*, Comput. Meth. Appl. Mech. Eng. **192** (2003), 941–954.
- [47] F. Soleymani, M. Barfeie, and F.K. Haghani, *Inverse multi-quadric RBF for computing the weights of FD method: application to American options*, Commun. Nonlinear Sci. Numer. Simul. **64** (2018) 74–88.
- [48] M. Tilenius, E. Larsson, E. Lehto, and N. Flyer, *A scalable RBF-FD method for atmospheric flow*, J. Comput. Phys. **298** (2015), 406–422.
- [49] A.I. Tolstykh, *On using RBF-based differencing formulas for unstructured and mixed structured-unstructured grid calculations*, Proc. 16th IMACSWorld Cong. **228**, 2000, pp. 4606–4624.
- [50] A.I. Tolstykh and D. A. Shirobokov, *On using radial basis functions in a "finite difference mode" with applications to elasticity problems*, Comput. Mech. **33** (2003), 68–79.
- [51] I. Tominec, P.F. Villard, E. Larsson, V. Bayona, and N. Cacciani, *An unfitted radial basis function generated finite difference method applied to thoracic diaphragm simulations*, J. Comput. Phys. **469** (2022), 111496.
- [52] G.B. Wright, *Radial basis function interpolation: Numerical and analytical developments*, Ph.D. thesis, University of Colorado, Boulder, CO, 2003.
- [53] G.B. Wright and B. Fornberg, *Scattered node compact finite difference-type formulas generated from radial basis functions*, J. Comput. Phys. **212** (2006), 99–123.
- [54] Y.H. Youssri, *Two Fibonacci operational matrix pseudospectral schemes for nonlinear fractional Klein–Gordon equation*, Int. J. Modern Phys. **33** (2022), no. 4, 2250049.